Quantitative Phosphoproteomics of Cytotoxic T Cells to Reveal Protein Kinase D 2 Regulated Networks*[S]

María N. Navarro‡¶, Juergen Goebel‡‖, Jens L. Hukelmann‡, and Doreen A. Cantrell‡§

The focus of the present study was to characterize the phosphoproteome of cytotoxic T cells and to explore the role of the serine threonine kinase PKD2 (Protein Kinase D2) in the phosphorylation networks of this key lymphocyte population. We used Stable Isotope Labeling of Amino acids in Culture (SILAC) combined with phosphopeptide enrichment and quantitative mass-spectrometry to determine the impact of PKD2 loss on the cytotoxic T cells phosphoproteome. We identified 15,871 phosphorylations on 3505 proteins in cytotoxic T cells. 450 phosphosites on 281 proteins were down-regulated and 300 phosphosites on 196 proteins were up-regulated in PKD2 null cytotoxic T cells. These data give valuable new insights about the protein phosphorylation networks operational in effector T cells and reveal that PKD2 regulates directly and indirectly about 5% of the cytotoxic T-cell phosphoproteome. PKD2 candidate substrates identified in this study include proteins involved in two distinct biological functions: regulation of protein sorting and intracellular vesicle trafficking, and control of chromatin structure, transcription, and translation. In other cell types, PKD substrates include class II histone deacetylases such as HDAC7 and actin regulatory proteins such as Slingshot. The current data show these are not PKD substrates in primary T cells revealing that the functional role of PKD isoforms is different in different cell lineages. ***Molecular & Cellular Proteomics 13: 10.1074/mcp.M113.037242, 3544–3557, 2014.***

The mammalian serine/threonine protein kinase D (PKD)[1] family comprises three different but closely related serine kinases, PKD1, PKD2, and PKD3 all of which have a highly conserved N-terminal regulatory domain containing two cysteine-rich diacylglycerol (DAG) binding domains (1). T lymphocytes express high levels of PKD2 and this kinase is selectively activated by the T-cell antigen receptor (TCR). The activation of PKD2 is initiated by DAG binding to the PKD N terminus but is also critically dependent on Protein kinase C (PKC)-mediated phosphorylation of two serine residues (Ser707 and Ser711) within the activation loop of the PKD2 catalytic domain (2, 3). The importance of PKD2 for T-cell function has been probed by experiments in mice that lack expression of catalytically active PKD2. These studies have shown that PKD2 is important for effector cytokine production after T-cell antigen receptor engagement and also for optimal induction of T-cell dependent antibody responses (4, 5). PKD2 thus has a key role in adult mice to control the function of T cells during adaptive immune responses.

The importance of PKD2 for primary T-cell function makes it critical to understand how PKD2 controls protein phosphorylation pathways. In this context, experiments with constitutively active and dominant negative PKD mutants in tissue culture cell lines have identified a number of candidate PKD substrates. These include the protein phosphatase Slingshot (6, 7), the Ras effector Rin1 (8), phosphatidylinositol-4 kinase III beta (9), lipid and sterol transfer proteins such as CERT and OSBP (10, 11). There are also experiments that have identified a key role for PKDs in regulating the phosphorylation and subcellular localization of the class II histone deacetylases (HDACs). For example, in PKD null DT40 B cell lymphoma cells the B cell antigen receptor cannot induce the phosphorylation and nuclear exclusion of the class II HDACs, HDAC5 and 7 (12). However, it remains to be determined whether the documented PKD substrates are universal PKD substrates in different cell lineages. In this context, the intracellular localization of PKD isoforms varies in different cells (13), and PKDs have also been shown to traffic between different cellular locations in response to specific stimuli (2, 14). PKD function

From the ‡Division of Cell Signalling and Immunology. College of Life Sciences University of Dundee, Dundee, Scotland, U.K.

⌘ *Author's Choice*—Final version full access.

Received, December 23, 2013 and in revised form, September 23, 2014

Published, MCP Papers in Press, September 29, 2014, DOI 10.1074/mcp.M113.037242

Author contributions: M.N.N., J.G., and D.A.C. designed research; M.N.N., J.G., and J.L.H. performed research; J.L.H. contributed new reagents or analytic tools; M.N.N. and D.A.C. analyzed data; M.N.N. and D.A.C. wrote the paper.

[1] The abbreviations used are: PKD, protein kinase D; CTL, cytotoxic T lymphocyte; DAG, diacylglycerol; HDAC, histone deacetylase; HILIC, hydrophilic liquid interaction chromatography; HPLC, high performance liquid chromatography; IL-2, interleukin 2; IMAC, immobilized metal ion affinity chromatography; MS, mass spectrometry; NFAT, nuclear factor of activated T cells; PKC, protein kinase C; SILAC, stable isotope labelling of aminoacids in culture; STAT, signal transducer and activator of transcription; TCR, T cell receptor; [Ca2+]i, intracellular Ca2+ concentration.

is dependent on its localization and cell context presumably reflecting that the localization of PKDs plays a key role determining the nature of PKD substrates in different cell populations (15).

Recently, mass-spectrometry based quantitative phosphoproteomics has been used to explore serine/threonine kinase controlled signaling pathways in T cells (16–18). In this regard, SILAC labeling combined with quantitative mass-spectrometry has recently been used to examine the impact of overexpressing active and/or kinase dead PKD1 mutants in HEK293 cells treated with nocodazole, a microtubule-depolymerizing reagent that disrupts the Golgi complex and activates PKD1 (19). This has identified a number of PKD1 substrates in HEK293 cells. PKD1 and PKD2 are highly homologous kinases but it remains to be determined whether the PKD1 substrates identified in nocodazole-treated HEK293 cells are relevant to signaling pathways controlled by endogenous PKD2 in antigen receptor activated primary T cells.

Accordingly, in the present study we used SILAC labeling combined with phosphopeptide enrichment and mass-spectrometry quantification to compare the phosphoproteome of antigen receptor activated wild type and PKD2 deficient cytotoxic T cells (CTLs). Our experiments identify and quantify more than 15,000 site-specific phosphorylations in antigen receptor activated CTLs and thus provide a unique data source about the signaling networks operational in these cells. The loss of PKD2 impacts on about 5% of these phosphorylations and reveals that PKD2 has both positive and negative regulatory roles in regulating protein phosphorylation networks in T cells.

EXPERIMENTAL PROCEDURES

Mice, Cell Culture, and SILAC Labeling—P14 T-cell receptor transgenic mice (P14-TCR) PKD2 null mice (4, 5), and wild-type littermates were bred and maintained under specific pathogen-free conditions in the Wellcome Trust Biocenter at the University of Dundee in compliance with U.K. Home Office Animals (Scientific Procedures) Act 1986 guidelines as previously describe (17, 20). P14 CTL were generated and labeled in SILAC media as previously described (17). Briefly, splenocytes were activated for 2 days with the P14-TCR cognate ligand (peptide gp33–41 from Lymphocytic Choriomeningitis Virus, LCMV). Then, cells were cultured for 4 days in SILAC medium (Dundee Cell Products, Dundee, UK), L-proline 200 mg/l, L-arginine 84 mg/l, pre-supplemented with 300 mg/l L-glutamate, 10% dialyzed FCS with a 10kDa cutoff (Invitrogen, Carlsbad, CA), 50 units/ml penicillin-G, 50 μg/ml streptomycin and 50 μM β-mercaptoethanol, and 20 ng/ml IL-2 (Proleukin, Novartis, Basel, Switzerland). The following arginine and lysine isotopes were used:

R0K0 (light): L − [$^{12}C_6$, $^{14}N_4$] arginine (R0)

and L − [$^{12}C_6$, $^{14}N_2$] lysine (K0)

R10K8 (heavy): L − [$^{13}C_6$, $^{15}N_4$] arginine (R10)

and L − [$^{13}C_6$, $^{15}N_2$] lysine (K8)

The SILAC labeling was performed in three biological replicates, where the P14 wild-type CTLs cells comprised the "light" condition and PKD2 null CTLs were labeled with "heavy" amino acids in two experiments (experiments 1 and 2), and a label switch was performed in the third experiment (experiment 3).

For the generation of non-TCR transgenic CTLs, splenocytes were activated for 2 days with 0.5 μg/ml of anti-CD3 antibody (2C11, R&D Systems, Minneapolis, MN), followed by 4 days of culture in RPMI (Life Technologies), 10% FCS (Invitrogen), supplemented with penicillin-G, streptomycin, β-mercaptoethanol, and IL-2.

Sample Preparation, Phosphopeptide Enrichment, and Mass Spectrometry—P14 wild-type and PKD2 null CTLs differentially labeled in SILAC media for 4 days were mixed at 1:1 ratio (total 3×10^8 cells) and stimulated for 5 min with P14-TCR cognate peptide (LCMV gp33–41). After TCR stimulation, cells were washed once in cold PBS and were subjected to cytosol and nuclear fractionation as previously described (17). Briefly, cells were resuspended in hypotonic lysis buffer (10 mM HEPES, pH 7.9, 15 mM KCl, 4 mM $MgCl_2$, 0.1 mM EDTA, 10 mM NaF, 0.15% (v/v) Nonidet-P40, 1 mM phenylmethylsulfonyl fluoride, 1 mM Na3VO4, and 1 mM dithiothreitol) and centrifuged for 1 min at 10,000 $\times$ g. Cytosolic fractions were removed and nuclear-membrane fractions were resuspended in nuclear lysis buffer (10 mM Tris, pH 7.05, 50 mM NaCl, 30 mM sodium pyrophosphate, 50 mM NaF, 5 mM ZnCl2, 10% (v/v) glycerol, and 0.5% (v/v) Triton-X100). Cytosolic and nuclear fractions were precipitated with trichloroacetic acid (10%, v/v) for 15 min/ice. Protein pellets were resuspended in Urea 8 M Tris-HCl 100 mM. Cytosolic and nuclear lysates were subjected to alkylation with iodoacetamide prior to trypsin digestion (Roche, Basel, Switzerland).

Hydrophilic Liquid Interaction Chromatography (HILIC), Immobilized Metal Ion Affinity Chromatography (IMAC), and Titanium Dioxide (TiO_2) Affinity Chromatography—Proteolytic digestion products were desalted on a 1-g Sep-Pak cartridge (Waters, Milford, MA), and subjected to hydrophilic interaction liquid chromatography (HILIC) using a 4.6 $\times$ 250-mm TSKgel Amide-80 5-μm particle column (Tosoh Biosciences, Tokyo, Japan). The following buffers were used: HILIC buffer A (0.1% TFA) and HILIC buffer B (99.9% acetonitrile and 0.1% TFA). The peptide pellets were resuspended in 80% HILIC buffer B and injected onto the HILIC column. The chromatography was done using the following elution gradient: 80% B held for 20 min followed by 80% B to 60% B in 40 min and finally 0% B for 10 min.

Eighteen fractions of each subcellular compartment were collected throughout the gradient and further enriched in phosphopeptides by immobilized metal affinity chromatography (IMAC, Phos-Select, Sigma) following manufacturer's instructions. Peptides were eluted with 200 μl, 0.4 M NH4OH followed with 200 μl, 0.2 M NH4OH/50% acetonitrile. A gel-loading tip was used to remove elution fractions and further remaining IMAC beads were removed by passing fractions through a ZipTip (Millipore). The supernatants from the IMAC (combining the 18 fractions for each subcellular compartment in nine samples) were used for additional TiO_2 pull down (Titanspheres, GL Sciences, Shinjuku, Japan).

Liquid Chromatography - Mass Spectrometry (LC-MS)—The peptide mixture was separated by nanoscale C18 reverse-phase liquid chromatography (Ultimate 3000 nLC (Dionex, Sunnyvale, CA) coupled online to a Linear Trap Quadrupole (LTQ)-Orbitrap mass spectrometer (LTQ-Orbitrap Velos; Thermo Fisher Scientific). The following buffers were used: HPLC Buffer A (2% acetonitrile and 0.01% formic acid), HPLC Buffer B (90% acetonitrile and 0.08% formic acid) and HPLC Buffer C (0.05% trifluoroacetic acid). Samples were injected in 1% formic acid, washed onto the column with HPLC Buffer C and eluted with a flow of 0.3 μl/min under usage of the following buffer gradient:

5% B (0–3 min), 5–35% B (3–68 min), 35–90% B (68–70 min), 90% B (70–80 min), 90–5% B (80–81 min), and equilibrated in 5% B (81–100 min). The eluting peptide solution was automatically (online) electrosprayed into the mass spectrometer using a nanoelectrospray ion source (Proxeon Biosystems, Odense, Denmark). The mass spectrometers were operated in positive ion mode and used in data-dependent acquisition modes. A full scan (FT-MS) was acquired at a target value of 1,000,000 ions with resolution $r = 60{,}000$ over a mass range of 335–1800 amu (atomic mass unit). The ten most intense ions were selected for fragmentation in the LTQ Orbitrap Velos. Fragmentation in the LTQ was induced by collision-induced dissociation (CID) with a target value of 10,000 ions. For accurate mass measurement, the "lock mass" function (lock mass = 445.120036 Da) was enabled for MS scan modes. To improve the fragmentation of phosphopeptides, the multistage activation algorithm in the Xcalibur software was enabled for each MS/MS spectrum using the neutral loss values of 48.99, 32.66, and 24.50 *m/z* units. Former target ions selected for MS/MS were dynamically excluded for 300 s. General mass spectrometric conditions were as follows: spray voltage, 1.0–2.5 kV; no sheath and auxiliary gas flow; ion transfer tube temperature, 150–180 °C; and normalized collision energy (35%) using wide band activation mode for MS2. The isolation width was set to 2 amu for IT-MS/MS. Ion selection thresholds were 600 counts for MS2. An activation of $q = 0.25$ and activation time of 30 ms were applied in MS2 acquisitions. The fill time for FTMS was set to 1000 ms and for ITMS to 150 ms. In this study, three independent biological replicates of P14 wild-type *versus* PKD2 knockout CTLs were analyzed, with two technical replicates for each biological sample (total 310 HPLC-MS/MS runs). In two experiments, the wild-type cells comprised the "light" condition, whereas the PKD2 knockout CTLs were labeled with "heavy" amino acids (experiments 1 and 2). In the third experiment, we performed a label switch (experiment 3).

Data Processing—For data analysis, we combined the raw data obtained from the two technical replicates, the two subcellular fractions (nucleus and cytosol), and the IMAC and TiO_2 phosphopeptide enrichment methods in each independent replicate. Data was processed using MaxQuant (21) version 1.3.0.5 which incorporates the Andromeda search engine (22). Proteins were mapped to the Uniprot mouse protein database ("Mouse Complete Proteome" retrieved on August 19, 2013). This version of the database contains 16,618 mouse complete proteome entries (UniProtKB/Swiss-Prot canonical and isoform sequence data). Search parameters specified an MS tolerance of 20 ppm, an MS/MS tolerance at 0.5 Da and full trypsin specificity, allowing for up to two missed cleavages. Carbamidomethylation of cysteine was set as fixed modification and oxidation of methionines, N-terminal protein acetylation, and phosphorylation of serine, threonine, and tyrosine were set as variable modifications. Peptides were required to be at least six amino acids in length with false discovery rates (FDRs) of 0.01 calculated at the level of peptides, proteins, and modification sites based on the number of hits against the reversed sequence database.

To make our data accessible to the scientific community, the MS proteomics data have been deposited to the ProteomeXchange Consortium (http://proteomecentral.proteomexchange.org) via the PRIDE partner repository (23) with the data set identifier PXD001076. The annotated_spectra.zip file contains .pdf files with annotated MS/MS spectra for all PTM containing peptides described in the manuscript. Separate MS/MS spectra for the highest identification and localization scores have been deposited. To facilitate the search for the annotated spectra, an additional excel file (Phospho (STY)Sites_annotated_spectra.xlsx file) containing a list of all reported sites and the file names of their corresponding .pdf files have been deposited. Prior to statistical analysis, the outputs from MaxQuant were filtered to remove known contaminants and reverse sequences. The distribution of SILAC ratios was normalized within MaxQuant at the peptide level so that the median of $\log_2$ ratios is zero (21) (supplemental Table S1).

Bioinformatics and Statistical Tools—For functional pathway analysis, the different subsets of proteins identified in the data set were subjected to functional analysis using DAVID bioinformatics resources (24). Gene ontology terms for biological processes (BP) and molecular functions (MF) charts were obtained using default statistical parameters (threshold: count 2, ease 0.1). Proteins with protein kinase activity and transcription factor activity were filtered based on GOTERM_MF_FAT (GO:0004672 and GO:0003700, respectively).

For the kinase motif distribution, Linear Motif analysis tool in Perseus v1.4.1.3 software was used. Significance of PKD2 motif enrichment was assessed by Chi-square test using Graphpad software (http://www.graphpad.com/).

Western Blotting—Protein expression was assessed using standard Western blotting protocols described elsewhere (5). Blots were probed with rabbit polyclonal anti-phospho-Cofilin-Ser3 and anti-Cofilin (Cell Signaling Technology, Danvers, MA), a rabbit polyclonal antisera recognizing HDAC7 (H-273, Santa Cruz Biotechnology, Santa Cruz, CA), or a mouse monoclonal anti-Erk1/2 antibody (3A7, Cell Signaling Technology) as indicated. Horseradish-peroxidase couple anti-rabbit and anti-mouse antibodies were purchased from Jackson Immunoresearch, West Grove, PA.

Retroviral Transduction, Confocal Microscopy, and Flow Cytometry—GFP-HDAC7 retrovirus was produced and P14 wild-type and PKD2 deficient CTLs were transduced as described (17, 25). Cells were adhered to coverslips coated with poly-l-lysine (Sigma-Aldrich), then fixed for 30 min at 25 °C with 4% (w/v) paraformaldehyde. A Zeiss LSM700 confocal microscope with an alpha Plan-FLUAR 100× objective (numerical aperture, 1.45) was used for confocal microscopy. For flow cytometry analysis, cells were stained as described (5). Fluorescein isothiocyanate-anti-CD8 (clone 53–6.7), phycoerythrin-anti-CD5 (clone 53–7.3) and allophycocianine-anti-CD25 (clone PC61) were purchased from BD Pharmingen. Data were acquired on a FACSCalibur (Becton Dickinson) and were analyzed with FlowJo software (Treestar, Ashland, OR).

RESULTS

The CTL Phosphoproteome—The present screen used SILAC-based quantitative phosphoproteomic analysis to characterize the kinase-substrate signaling networks present in antigen receptor activated cytotoxic T cells (CTL). SILAC labeling requires that cells undergo multiple cell doublings to ensure sufficient label penetrance. Accordingly, for SILAC experiments in CD8 T cells we used a well-characterized model of CD8 CTL differentiation (17). In this model, antigen primed $CD8^+$ T cells from P14 TCR transgenic mice are cultured in interleukin 2 (IL-2) to produce a homogenous population of fully differentiated effector CTL (20, 26, 27). This model reproduces the *in vivo* situation where sustained IL-2 signaling promotes the production of terminally differentiated effector CTLs required for virus clearance (28–30). The impact of loss of the serine-threonine kinase PKD2 on CTL signaling networks was also explored. Hence, in these experiments wild-type or PKD2 knockout P14-TCR CTLs were differentially labeled with one of two different isotope combinations of lysine (K) and arginine (R), R0K0 ("light") and R10K8 ("heavy"). After 4 days of culture in SILAC media, wild-type and PKD2 knockout CTLs were mixed at equal cell number and triggered via their TCR with cognate peptide for 5 min to maximally

activate PKD2 in the wild-type population. Cells were then lysed, digested with trypsin and phosphopeptides were enriched by HILIC fractionation followed by IMAC and TiO_2 affinity chromatography. The workflow of our experiments is displayed in Fig. 1*A*. The phosphopeptide-enriched fractions were analyzed in a LTQ-Orbitrap Velos for mass spectrometry (MS) data collection. All raw mass spectrometry data from three biological replicates were processed using the MaxQuant software.

A key aim of this study was to map the repertoire of protein phosphorylations in CTLs. The collective analysis of the current experiments identified and quantified 15,871 unique phosphorylation sites in CTLs on 3505 distinct proteins. The full list of all unique phosphosites identified in our analysis can be found in supplemental Table S1. The ratio of phosphorylations on Serine, Threonine, and Tyrosine residues was 81/17/2, comparable to what has been observed in other phosphoproteomic studies (31, 32). Importantly, the total number of phosphosites identified in the individual biological replicates was similar (Fig. 1*B*), and ~58% of the unique phosphosites (9205 on 2767 proteins) were identified in all three replicates (Fig. 1*C*). We have previously described a phosphoproteomic analysis of CTLs but these earlier experiments only identified 2000 phosphorylations in CTLs (17). The higher coverage obtained in the present set of experiments offers a more complete view of CTL signaling networks.

We used DAVID Bioinformatics Resources 6.7 (24) to perform functional pathway analysis on the phosphoproteins and found that the CTL phosphoproteome is significantly overrepresented by proteins that control gene transcription and chromatin and by kinases and phosphatases that control protein phosphorylation (Fig. 1*D*). There was also overrepresentation in the CTL phosphoproteome of molecules that regulate macromolecular catabolic processes, notably proteins that control the ubiquitylation and sumoylation of proteins (Fig. 1*D*). The mouse genome encodes over 500 protein kinases (33). The present data detected phosphopeptides from ~200 protein kinases in CTLs (supplemental Table S2). We have also used Linear Motif analysis tool in Perseus software to assign the kinases most likely to phosphorylate the 15,871 phosphosites identified in CTLs. This work indicated activity of a minimum of 54 serine/threonine kinases and eight tyrosine kinases in CTLs (Fig. 1*E*). One limitation of this latter analysis is that is difficult to assign substrates individually to closely related kinase isoforms that may share substrate specificity. For example, a proportion of the identified phosphosites in CTLs was predicted to be phosphorylated by Protein Kinase A (PKA) or Protein Kinase C (PKC) (Fig. 1*E*). These are members of the AGC family of kinases and it is very likely that substrates assigned to PKA or PKC may in fact be phosphorylated by other AGC kinases. In this context, the present data reveals the full repertoire of AGC kinase isoforms expressed in CTLs. For example, five of the possible nine Protein Kinase C isoforms were detected in CTLs, PKCα β, δ, PKCη, and PKCθ (Table I). The data presented in Table I show that AGC kinases in CTL also include two of the four RSK isoforms, RSK1 and RSK2; two of the three Akt isoforms, Akt1 and Akt2; one of the three serum glucocorticoid kinases, SGK3, and one of the two possible S6K isoforms, S6K1. In a similar way, the kinase prediction analysis also indicated activity of the adenosine monophosphate (AMP)-activated protein kinase in CTL (Fig. 1*E*). It is known that CTL are dependent for their survival on LKB1 (34), which phosphorylates and activates AMPKα1, AMPKα2, and 13 other AMPK-related kinases (AMPK-RK) (35). The deletion of AMPKα1 does not phenocopy the loss of LKB1 in T cells indicating that it must be other AMPK family members that mediate LKB1 actions (36). The present data identify the candidates to mediate LKB1 function in T cells, because CTLs express multiple AMPK family isoforms apart from AMPKα1 notably SNRK; SIK1 and 3, and MARK2, 3, and 4 (Table I). The data presented in Table I and supplemental Table S2 identifying the specific kinase isoforms expressed in CTLs offer invaluable knowledge in the context of the selection of isoform-specific inhibitors of kinase activity and the development of new inhibitors targeting T-cell function.

The relevance of kinase-substrate networks present in CTLs relies in their ability to dictate the transcriptional program controlling T-cell effector function during an immune response. Accordingly, the most overrepresented function among phosphorylated proteins in CTLs is the regulation of transcription (Fig. 1*D*). Of the 160 proteins with annotated transcription factor activity identified in our data set (supplemental Table S3), we found relevant phosphorylation sites that regulate transcriptional activity, subcellular localization, and/or protein stabilization of essential transcription factors for CTL development such as the STAT family members STAT3, STAT4, and STAT5, Foxo1, Foxo3, or Myc (Table II). More importantly, we identify phosphorylation sites in key transcription factors such as Eomes, T-bet, Hif1α, Arnt, Tfeb, Srebf1, and Srebf2 or Irf4 whose function has not been yet characterized (Table II). Notably, several of the phosphosites found for these transcription factors are predicted to be phosphorylated by kinases known to be active in antigen stimulated T cells such as Erk1/2, GSK3, or PKC family (Table II and supplemental Table S3). These data thus open the door for novel targeted approaches exploring the role of protein phosphorylation in regulating CTL transcriptional program.

Impact of PKD2 Deficiency on the Cytotoxic T-cell Phosphoproteome—A second aim of the present screen was to use SILAC-based quantitative phosphoproteomic analysis to explore the role of PKD2 in CTLs. The present data reveal that antigen activated CTLs have high levels of active PKD2. We found eight unique phosphosites derived from PKD2 in wild-type CTLs including peptides corresponding to phosphorylated residue Ser711 (Table III). This phosphorylation is mediated by PKCs and is critical for PKD2 catalytic activity (4). When active, PKD2 autophosphorylates on Ser873 (37); the presence of phosphorylated PKD2-Ser873 in CTLs thus con-

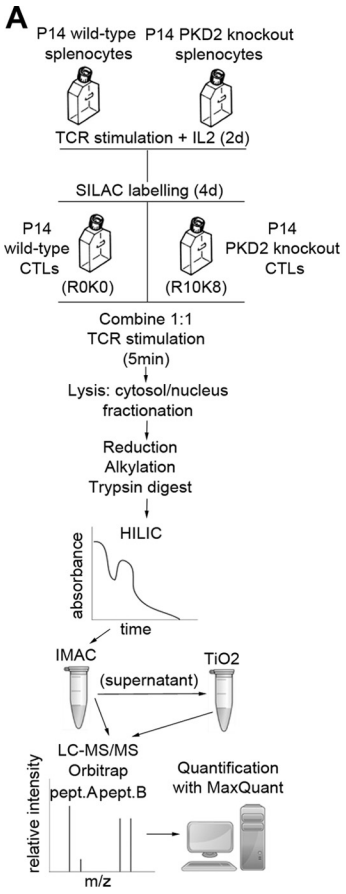

B

	n p-sites	n proteins
Exp. 1	11,301	2,962
Exp. 2	11,331	2,962
Exp. 3	14,185	3,346
Total	**15,871**	**3,505**

C

	% overlap	n p-sites overlap
Exp. 1-2	76.24	9,786
Exp. 1-3	66.45	10,170
Exp. 2-3	66.42	10180
Exp. 1-2-3	57.99	9,205

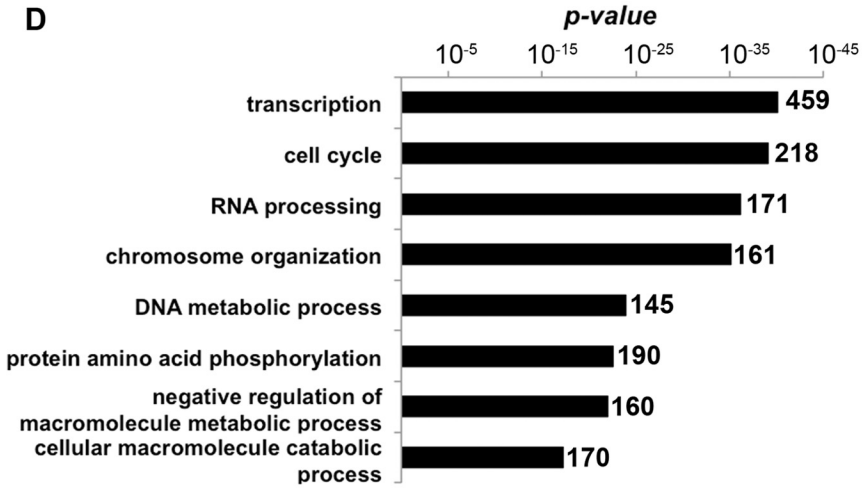

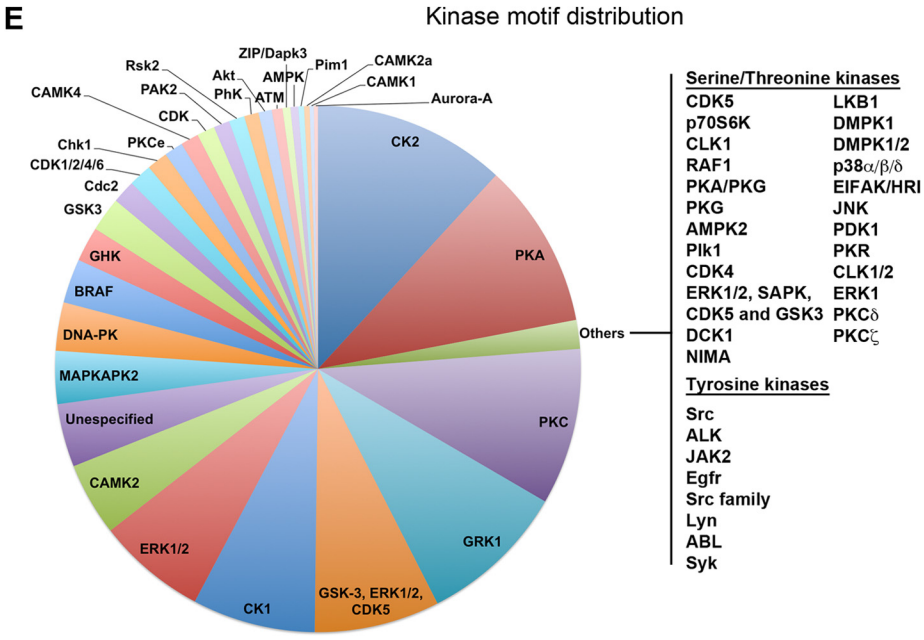

FIG. 1. **Global phosphoproteomic analysis of PKD2 deficient CTLs.** *A*, Experimental workflow. *B*, Number of unique phosphosites (p-site) and number of distinct proteins identified and quantified in the three individual biological replicates. *C*, Percentage and numbers of unique phosphosites (p-sites) identified in all three biological replicates. *D*, Graph represents the statistical significance (*p value*) of the biological processes overrepresented within the CTL phosphoproteome. Inset numbers indicate number of proteins in each group. *E*, Pie chart represents the frequency of kinases predicted to be active in CTLs.

TABLE I

AGC family and AMPK related kinases in CTLs. List of AGC and AMPK-related kinase family members identified in the CTL phosphoproteome

Kinase family	Kinase	Isoforms present in CTLs
AGC	PDK1	PDK1/*Pdpk1*
	PKC	PKCα/*Prkca*
		PKCb/*Prkcb*
		PKCθ/*Prkcq*
		PKCη/*Prkch*
		PKCδ/*Prkcd*
	PKN	PNK1/*Pnk1*
		PNK2/*Pnk2*
	Akt	Akt1/*Akt1*
		Akt2/*Akt2*
	S6K	S6K1/*Rps6kb1*
	RSK	RSK1/*Rps6ka1*
		RSK2/*Rps6ka3*
	SGK	SGK3/*Sgk3*
	PKA	PKAa/*Prkaca*
		PKAb/*Prkacb*
	MSK	Msk1/*Rps6ka5*
		Msk2/*Rps6ka4*
AMPK related kinases	AMPK	AMPKa1/*Prkaa1*
	SNRK	SNRK/*Snrk*
	SIK	SIK1/*Sik1*
		SIK3/*Sik3*
	MARK	MARK2/*Mark2*
		MARK3/*Mark3*
		MARK4/*Mark4*

TABLE II

Phosphosites in relevant CTL transcription factors. Identified phosphosites in selected transcription factors known to be essential for CTLs differentiation and function, presented as gene name and modified position (Mod. Pos.)

Gene name	Mod. Pos.
Stat3	S701; Y705; T714; T716; S727
Stat4	S714; S716; S722; S714; S716; S722
Stat5a	S127; S128; Y694; S773; S779; S791
Stat5b	S127; S128; Y699; S127; S128; Y699
Foxo1	S253; S284; S287; S295; S326; T330; S429; T464; S465; S467
Foxo3	S7; S12; S252; T260; S279; S285; S293; S296; S424
Myc	T58; S62; S64; S71; S73; Y74; S160; S164; S282; S288; S293
Eomes	S52; S117; S617; S667; S672; S676
Tbx21	S498; S506; S508; S514
Hif1a	S450; S679
Arnt	S45; S77; S82; S83
Tfeb	S108; S113; S121; S333; S465; S466
Srebf1	S96; S100
Srebf2	S458
Irf4	S186; T435; T436; S446; S447

firms the activity of this kinase in these cells (Table III). Importantly, the SILAC ratio for all the phosphosites found for PKD2 was down-regulated in PKD2 deficient CTLs, particularly the

TABLE III

PKD2 and PKD3 phosphosites. List of phosphosites derived from PKD isoforms detected in CTL phosphoproteome, presented as gene name, modified position (Mod. Pos.), sequence window (Seq. window) and SILAC ratio KO/WT (KO/WT ratio, averaged value of the three biological replicates)

Gene name	Mod. Pos.	Seq. window	KO/WT ratio
PKD2			
Prkd2	S197	ARKRRL**S**STSLAS	0.67
	S198	RKRRLS**S**TSLASG	0.43
	S200	RRLSST**S**LASGHS	0.48
	S211	HSVRLG**S**SESLPC	0.36
	S212	SVRLGS**S**ESLPCT	0.63
	S214	RLGSSE**S**LPCTAE	0.18
	S711	EKSFRR**S**VVGTPA	0.11
	S873	GLAERI**S**IL___	0.06
PKD3			
Prkd3	S31	APSPCS**S**PKTGLS	1.37
	S27	AVLPAP**S**PCSSPK	1.26
	S30	PAPSPC**S**SPKTGL	1.17
	S213	VRKRRL**S**NVSLPG	1.06
	S216	RRLSNV**S**LPGPGL	1.06
	S252	PSKRIP**S**WSGRPI	0.96
Prkd3;Prkd1	S391	ETVKTI**S**PSTSNN	1.07
	S395	TISPST**S**NNIPLM	0.97
	S730	RIIGEK**S**FRRSVV	0.79
	S734	EKSFRR**S**VVGTPA	0.79

C-terminal phosphosites (Table III). Previous studies have indicated that T cells do not express PKD1 and only express low levels of PKD3 (4). The current analysis found six phosphopeptides for PKD3, and another four whose sequence can be assigned to either PKD3 or PKD1. In addition, the data shows that there was no change in the SILAC ratio for PKD3 phosphosites in PKD2 deficient CTLs (Table III). Thus, the loss of PKD2 catalytic function in CTLs is not compensated by increased expression or activity of other PKD isoforms.

The PKD2 deficient mice used in the present study were generated by a retrovirus-based gene-trap technique, where the "gene-trap" insertion within the *Prkd2* locus was mapped to exon 15 encoding from amino acid 658 of PKD2 (4). PKD2 antibodies raised against the C-terminal portion of the protein (exons 16–18) have thus confirmed the loss of PKD catalytic activity in PKD2 "gene-trap" mice (4), but the possibility that a truncated N-terminal noncatalytic fragment of PKD2 protein might be expressed in the PKD2 "gene-trap" T cells has not been considered. The present data also show that phosphosites from the C terminus of PKD2 were down-regulated by more than 14-fold in the PKD2 "gene-trap," indicating that they are absent (Table III). However, phosphosites derived from the N terminus of PKD2 (S197, S198, S200, S211, and S212) showed a two- to threefold decrease in expression in PKD2 gene trap CTLs. These data argue that PKD2 "gene-trap" T cells still express a low level of a residual N-terminal fragment of PKD2 and confirm that they lack the PKD2 catalytic domain.

As mentioned above, CTL effector function is maintained by the integration of signals emanating from the TCR and the IL-2R. The SILAC ratio of wild-type and PKD2 deficient cells comparison displayed a normal distribution (Fig. 2*A*), suggesting that deletion of PKD2 did not skew the CTL phosphoproteome. In particular, there was not a general decrease in TCR regulated phosphorylations in PKD2 null cells. For instance, TCR triggering elevates intracellular calcium levels and induces calcium/calcineurin-regulated dephosphorylation of the transcription factor Nuclear Factor of Activated T cells c2 isoform (NFATc2) (17). PKD2 loss had no impact on NFATc2 phosphorylation (Table IV). There was also no evidence for loss of TCR mediated phosphorylation of the microtubule stabilizing protein Stathmin (*Stmn1*) on residues that are phosphorylated by Calcium/Calmodulin dependent kinase IV (Table IV). Moreover, triggering of the TCR phosphorylates AMPKα1 on Thr172 via a [Ca^{2+}]i-CaMKK pathway and AMPK Thr172 phosphorylation was normal in PKD2 null T cells (corresponding to *Prkaa1*-Thr183 in our data set, Table IV). It was also notable that the phosphorylation and activity of Erk1 and 2 was not influenced by PKD2 loss (*Mapk3* and *Mapk1*, respectively, Table IV). IL-2R signaling in CTLs induces high levels of active Akt and we noted normal levels of phosphorylated Akt substrate sites Ser253/Ser252 in Foxo1/3 respectively, indicating that Akt activity was normal in PKD2 null CTL (Table V). Moreover, IL-2 controls the tyrosine and serine phosphorylation of the transcription factors STAT3, STAT5a, and STAT5b in T cells (38, 39). These transcription factors were normally tyrosine and serine phosphorylated in PKD2 null CTL (Table V). Collectively, data in Table IV and V show that many CTL signaling pathways function normally in the absence of PKD2 catalytic function.

PKD2 Regulated Phosphorylations in CTL—There was some impact of PKD2 loss on the CTL phosphoproteome. Hence, of the 15,871 unique phosphosites identified and quantified in CTLs, 450 phosphosites on 281 distinct proteins were down-regulated and 300 phosphosites on 196 proteins were up-regulated in PKD2 null CTLs (Fig. 2*B*). The threshold for change was set to a z-core of 2 for phosphorylation ratios in PKD2 null *versus* wild-type CTLs, using the averaged value of the three biological replicates (1.8-fold change). We discarded phosphorylation events that displayed an inconsistent trend in regulation among the three biological replicates (*i.e.* down-regulated in one replicate and up-regulated in another). Based on this threshold, the data showed that PKD2 directly and indirectly regulates about 5% of the phosphorylations of cytotoxic T cells, on proteins that are mainly involved in transcription, chromosome reorganization and more importantly in the context of cytotoxic T cells, in leukocyte activation and hemopoiesis (Fig. 2*C*).

Among the down-regulated sites implicated in leukocyte activation we found five phosphosites derived from CD5 (Fig. 2*D*), a cell surface glycoprotein whose expression is normally increased after activation in T cells (40). This could reflect loss of CD5 phosphorylation or loss of CD5 expression. In this respect we have established that PKD2 controls expression of CD5 during T-cell development (15) but its role in controlling CD5 expression in peripheral T cells is unknown. Accordingly, we used flow cytometry to examine if CD5 expression was impaired in PKD2 deficient CTLs. Data in Fig. 2*E* show that PKD2 deficient CTLs express lower levels of CD5 than their wild-type counterparts.

We also found two down-regulated phosphosites derived from the F-actin severing protein Cofilin, Ser3, and Ser41, in the TCR activated PKD2 null CTL (Fig. 2*F*). This result was initially surprising as previous studies have shown that TCR triggering, which activates PKD2, normally down-regulates Cofilin-Ser3 phosphorylation (17). Indeed, Western blot experiments confirmed that TCR triggering reduces Cofilin-Ser3 phosphorylation in CTLs (Fig. 2*G*). Nevertheless, there was strikingly less phosphorylated Cofilin-Ser3 in the both non-stimulated and TCR stimulated PKD2 null T cells compared with wild-type cells (Fig. 2*G*). These data orthogonally validated the reduced Cofilin-Ser3 phosphorylation in the TCR activated PKD2 null T cells observed in the mass spectrometry experiments (Fig. 2*F*, *G*). The reduced Cofilin phosphorylation in PKD2 null T cells argues that PKD might control the activity of kinase pathways upstream Cofilin phosphorylation. In this respect, previous studies have reported a PKD requirement for the phosphorylation of Ser3 on Cofilin via PKD activation of PAK4/LIMK (41, 42).

To search for PKD2 substrate candidates within the data set we used the following criteria: the SILAC ratio must be down-regulated in the PKD2 null cells, and the sequence of the down-regulated phosphosite must correspond to a PKD2 consensus motif. The consensus sequence for PKD2 phosphorylation described in the literature is (L/V/I)x(R/K)xx(S*/T*) (43–45). In addition to the described consensus site, PKD2 has an auto-phosphorylation site at residue Ser873 (Ser916 in PKD1) (37). This PKD2 autophosphorylation motif has slightly modified sequence compared with the conventional motif, (L/I)xx(R/K)x(S*/T*), but because it is a well described substrate for PKD2 we have included this sequence in our search for PKD2 phosphorylation sites. The analysis of the whole data set determined that among the 15,871 phosphosites found in our study, 940 contained a consensus motif for PKD2 phosphorylation (6% of the data set) (supplemental Table S1). Strikingly, 73 out of the 450 phosphosites (16%) with decreased phosphorylation in PKD2 deficient CTLs had a PKD2 consensus motif, whereas only 26 out of the 300 phosphosites (9%) with increased phosphorylation matched the PKD2 consensus motif (Fig. 2*H*). Thus among the down-regulated phosphosites in PKD2 knockout CTLs, we had a significant enrichment of phosphosites containing a consensus phosphorylation site for PKD2 ($p < 0.0001$, Fig. 2*I*). Detailed information about modified position and ratios of the 73 phosphosites on 69 distinct proteins down-regulated in our data set that had a PKD2 consensus motif can be found in

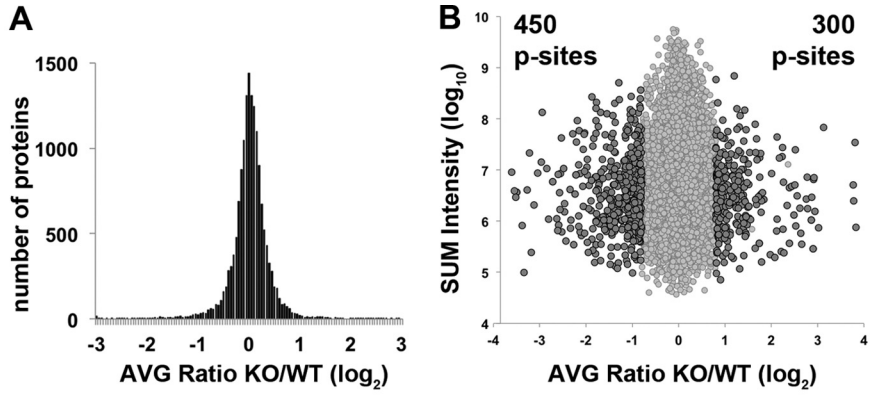

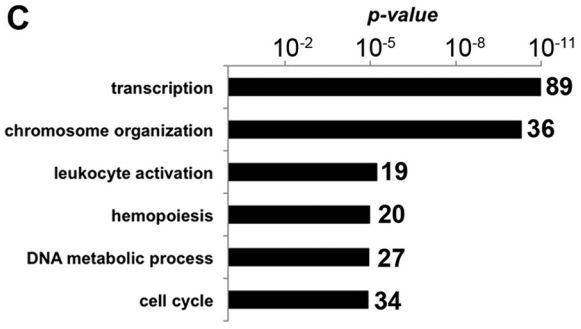

D

Gene name	Mod. Pos.	KO/WT ratio
Cd5	S427	0.24
	T433	0.16
	S438	0.24
	S481	0.24
	S482	0.27

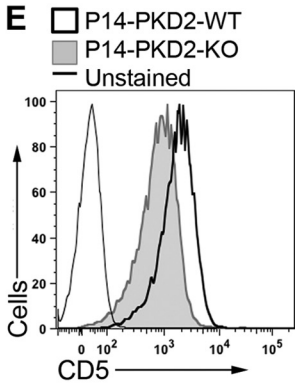

F

Gene name	Mod. Pos.	KO/WT ratio
Cfl1	S3	0.46
	S23	1.00
	S24	0.93
	T25	0.88
	S41	0.38

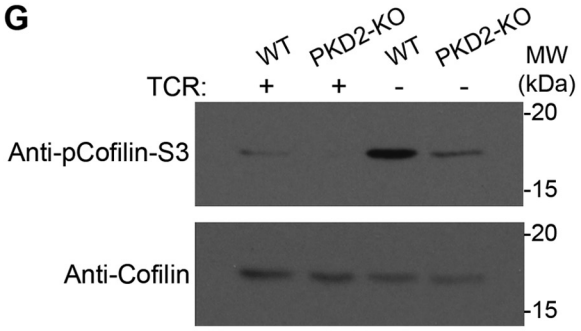

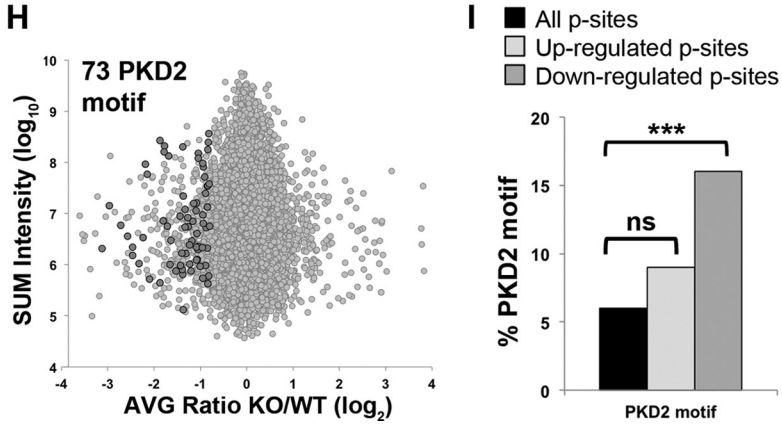

FIG. 2. **Impact of loss of PKD2 in the CTL phosphoproteome.** *A*, Histogram shows the SILAC ratio distribution of the data set, using the averaged SILAC ratio of the three biological replicates (PKD2 knockout *versus* wild-type, AVG KO/WT, $\log_2$ value). *B*, Graph shows SILAC ratio distribution (AVG KO/WT, $\log_2$ value) plotted against the signal intensity (sum of intensities of the three biological replicates, $\log_{10}$) for all identified phosphopeptides. Dark dots and inset numbers indicate phosphosites (p-sites) with a z-score of 2 (1.8-fold change). *C*, Graph

TABLE IV
T-cell receptor regulated phosphosites. Selected phosphosites known to change phosphorylation status after TCR stimulation, presented as gene name, modified position (Mod. Pos.) and SILAC ratio KO/WT (KO/WT ratio, averaged value of the three biological replicates)

Gene name	Mod. Pos.	KO/WT ratio
Nfatc2	S136	0.99
	S238	0.74
	S270	0.50
	S365	1.40
	S369	1.53
	S757	0.98
Stmn1	S16	0.90
	S25	0.92
	S38	0.82
	S63	0.93
Prkaa1	T183	1.04
Mapk3	T203	1.18
Mapk1	T179	1.00
	T183	0.99

TABLE V
Interleukin 2 regulated phosphosites. Selected phosphosites known to change phosphorylation status after IL-2 stimulation, presented as in Table IV

Gene name	Mod. Pos.	KO/WT ratio
Stat3	Y705	1.73
	S727	1.33
Stat5a	Y694	0.88
	S779	1.24
Stat5b	Y699	0.90
Akt1	S473	0.82
Akt2	S474	0.96
Foxo1	S253	0.98
Foxo3	S252	0.97

supplemental Table S4. It was notable that 377 of the 450 phosphosites with decreased phosphorylation in PKD2 deficient CTLs, including Cofilin1-Ser3 (Fig. 2*E*), did not have a consensus PKD2 site and hence are unlikely to be directly phosphorylated by PKD2 (Fig. 2*B*, 2*F*). In addition, loss of PKD2 increased the phosphorylation of 300 phosphosites (Fig. 2*B*) and this is clearly an indirect consequence of PKD2 loss.

Table VI lists the 69 proteins phosphorylated on a PKD2 consensus sequence whose phosphorylation was decreased in PKD2 null T cells. It also lists the biological function ascribed to these proteins. The decreased phosphorylation of these proteins in PKD2 null cells could reflect that they are direct substrates for PKD2. However, it is possible that the expression of the protein is decreased. To attempt discriminate between these possibilities, we analyzed all the phosphosites found in our study for the proteins presented in Table VI. For 41 proteins we could find evidence that although they had lost phosphorylation on PKD consensus sequences there were other phosphorylation sites that were unchanged, indicating that the protein expression was not decreased. For 22 proteins only one to two phosphosites were found and hence we cannot make any conclusion about their expression. However, for another four proteins, HDAC7, Osbl3, Sgk223, and Specc1, there was decreased phosphorylation of all detected peptides derived from these proteins (supplemental Table S1). This could indicate that there is lower expression of these proteins in PKD2 deficient CTLs. This second group included histone deacetylase HDAC7 (Table VI), which is a well characterized PKD substrate in many cells including B cells (12, 46). Moreover, in CTLs, HDAC7 phosphorylation on PKD consensus sites is essential for HDAC7 nuclear exclusion (17). HDAC7 is thus a very strong candidate for a PKD2 substrate in CTLs. However, Fig. 3*A* shows that the loss HDAC7 phosphorylation in PKD2 null CTLs occurred on multiple sites and was not restricted to the PKD substrate sequences Ser156 and Ser182 (47, 48). We therefore explored the possibility that PKD2 knockout CTLs may have decreased expression of HDAC7. The Western blot in Fig. 3*B* addresses this question and shows that PKD2 knockout CTLs express lower levels of HDAC7 compared with wild-type CTLs. The decrease in HDAC7 phosphorylation in PKD2 null CTL thus reflects that these cells have reduced expression of this molecule. In this respect, nonphosphorylated HDAC7 would accumulate in the nucleus whereas phosphorylated HDAC7 is in the cytosol (17). Confocal microscopy comparing the intracellular location of HDAC7 in wild-type and PKD2 deficient CTLs clearly showed that HDAC7 localization is mainly cytosolic in both wild-type and PKD2-deficient CTLs (Fig. 3*C*). HDAC7 phosphorylation on PKD consensus sites is also essential for CTL to express the IL-2Ralpha chain (CD25) (17). Fig. 3*D* shows that PKD2 deficient cells express normal levels of CD25. These data collectively argue that HDAC7 is not a PKD2 substrate in cytotoxic T cells.

represents the statistical significance (*p value*) of the biological processes overrepresented among the proteins with down-regulated and up-regulated phosphosites in PKD2 deficient CTLs. Inset numbers indicate number of proteins in each group. *D*, Phosphosites derived from CD5 (*Cd5*), presented as gene name, modified position (Mod. Pos.) and SILAC ratio KO/WT (KO/WT ratio, averaged value of the three biological replicates). *E*, Flow cytometry analysis of CD5 cell surface expression in P14 wild-type (P14-PKD2-WT) and PKD2 knockout (P14-PKD2-KO) CTLs. *F*, Phosphosites derived from Cofilin (*Cfl1*), presented as gene name, modified position (Mod. Pos.) and SILAC ratio KO/WT (KO/WT ratio, averaged value of the three biological replicates). *G*, Western blot analysis of wild-type and PKD2 knockout (WT and PKD2-KO) CTLs after 5 min of antigen receptor stimulation (TCR), using anti-phospho-Cofilin-Ser3 and anti-Cofilin antibodies. *H*, Graph shows SILAC ratio distribution plotted as in 2*B* for all identified phosphopeptides. Dark dots and inset number indicate phosphosites with at least 1.8-fold down-regulation that contain a PKD2 consensus motif (PKD2 motif). *I*, Frequency of PKD2 consensus motifs among all, up- and down-regulated phosphopeptides. Asterisks indicate significance of PKD2 motif enrichment (*** = $p < 0.0001$, Chi-square test).

TABLE VI

Functional annotation of PKD2 substrate candidates. 73 PKD2 substrate candidates involved in the indicated cellular functions were categorized based on available literature

Intracellular transport				Lymphocyte signaling
Small GTPase regulators	Cytoskeleton regulation	Endocytosis	Golgi function	
Arhgap11a	Arhgef2	Akap10	Dennd5a	Casp8ap2
Arhgef2	Arpc1b	Arl14ep	Lrmp	Cbl
Kifap3	Lpp	Cbl	Osbpl3	Hsh2d
Rin3	Map4	Hip1r	Ssr3	Ikbke
Tsc2	Ndrg1	Kifap3		Inpp4b
	Ospl3	Ndrg1		Ndrg1
	Plec	Reps1		Plekha2
	Rin3	Snx2		Prrc2a
	Tjp3	Snx9		Ptpn22
	Vim	Tbc1d5		Sgk223
	Wnk1	Ube2o		Tsc2
		Vps26b		

Gene expression				Other functions
Chromatin regulation	Transcription	Translation	Ubiquitin ligases	
Arid4b	Casp8ap2	Bud13	Cbl	Ccdc92
Arid5b	Lpp	Farsa	Dcaf5	Dmwd
Hdac5	Lrrfip1	Nup214	Rnf213	Dnajc8
Hdac7	Nfatc3	Pcbp1	Ube2o	Fam76b
Kansl3	Pola2	Phax		Specc1
Kdm2a	Polk	Rpl19		
Setdb1	Rdbp	Sugp2		
Sfr1	Supt16h			
	Trim28			
	Ylpm1			
	Znf280d			
	Zfp687			

The data presented for HDAC7 is thus a good demonstration of how decreased phosphorylation of a protein in a particular cell may be because of the fact its expression is decreased. Nevertheless, in the current data set there were at least 41 proteins that had decreased phosphorylation on PKD substrate sequences yet phosphorylations on other sites were unchanged, making these strong candidates to be PKD2 substrates (Table VII). Six of these proteins, Hip1r, Map4, Rdbp, Ssr3, Snx2, and Pcbp1, have been shown to be *in vitro* substrates for PKD1 (19) (Tables VI and VII). We also identified Rin3 (Ras and Rab interactor 3) as a PKD2 substrate (Tables VI and VII) and previous studies have identified Rin1 as a PKD1 substrate in fibroblasts (49). It was, however, important that our studies identified novel PKD2 substrate candidates in CTLs such the E3 ubiquitin ligase c-Cbl (*Cbl*) (50), the Lysine (K)-specific demethylase 2a (*Kdm2a*) (51), the transcription factor NFAT3 (52) and the Phosphorylated adaptor for RNA export (*Phax*), a regulator of U snRNA nuclear export (53).

DISCUSSION

The present study explores the phosphoproteome of antigen receptor activated cytotoxic T lymphocytes and identifies 15,871 unique phosphorylation sites on 3505 distinct proteins in this critical lymphocyte population. This is a unique data set about the kinase-substrate signaling networks in CTL that allows new insights about the repertoire of protein kinases that are expressed and active in T cells. One new vision derived from this work is that the CTL phosphoproteome was overrepresented by proteins that regulate macromolecular catabolic processes, notably proteins that control the ubiquitylation and sumoylation. In this respect, the reversible ubiquitin or sumo modification of proteins is critical for intracellular signal transduction pathways (54, 55). Moreover, it has been recognized for several years that cross talk between phosphorylation and ubiquitylation/sumoylation signaling occurs (56, 57). For example, phosphorylation of various E3 ligases can either positively or negatively regulate their deubiquitylation activity (56). The phosphorylation of a protein can create a docking site for a particular E3 ligase whereas in other cases, phosphorylation controls the intracellular localization of E3 ligases and their substrates (56). The full extent of the cross talk between protein phosphorylation and ubiquitylation is not understood in any cell system. However, the overrepresentation in the CTL phosphoproteome of molecules linked to the control of ubiquitylation and sumoylation signaling is a striking indication that the intersection between different post-transcriptional modifications may be critical to control CTL function.

The study also presents an exhaustive analysis of the impact of the loss of a single kinase, PKD2, in CTLs using an unbiased phosphoproteomic approach. This global analysis allows the characterization of direct and indirect PKD2-regu-

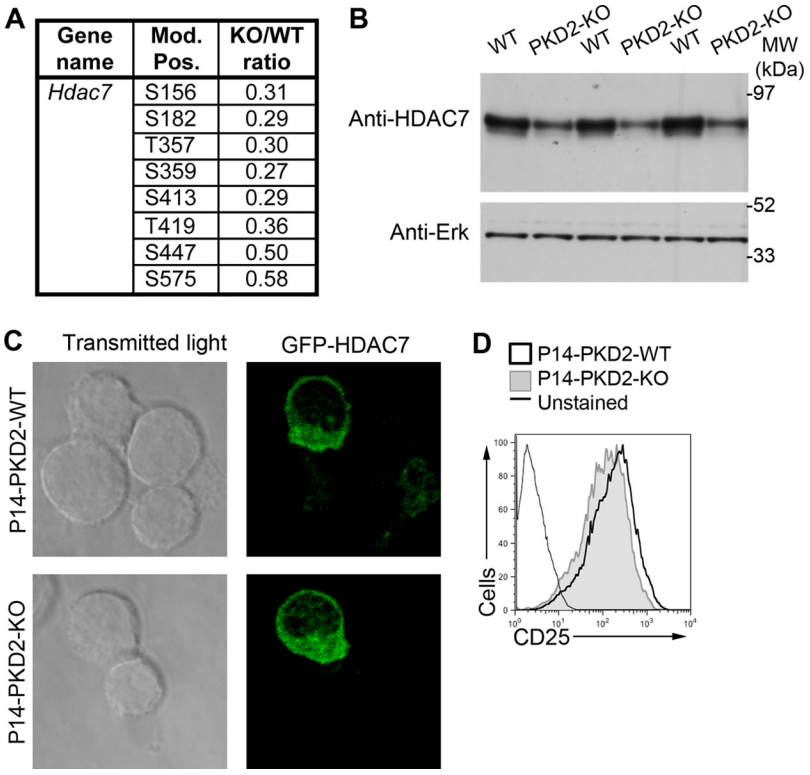

FIG. 3. **Analysis of HDAC7 phosphorylation, expression and function in PKD2 deficient CTLs.** *A*, Phosphosites derived from HDAC7 (*Hdac7*), presented as gene name, modified position (Mod. Pos.) and SILAC ratio KO/WT (KO/WT ratio, averaged value of the three biological replicates). *B*, Western blot analysis of three sets of wild-type and PKD2 knockout (WT and PKD2-KO) CTLs using an anti-HDAC7 antibody. Anti-Erk1 antibody was used as a control of equal loading. *C*, Microscopy analysis of the subcellular distribution of GFP-HDAC7 in retrovirally transduced P14 wild-type (P14-PKD2-WT) and PKD2 knockout (P14-PKD2-KO) CTLs. Original magnification, ×100. *D*, Flow cytometry analysis of CD25 cell surface expression in P14 wild-type (P14-PKD2-WT) and PKD2 knockout (P14-PKD2-KO) CTLs.

lated phosphorylation events. CTL express a minimum of 200 kinases yet the loss of a single kinase can have complex direct and indirect effects on the phosphoproteome. A single kinase PKD2 thus directly and indirectly regulates about 5% of CTL phosphorylations. Proteins identified as PKD2 substrates in CTLs include proteins involved in two distinct biological functions: regulation of intracellular protein trafficking and control of different aspects of gene expression. In the context of vesicular trafficking, the proteins phosphorylated by PKD2 in CTLs include a number of Rab GTPases regulators such as Akap10 (58), Tbc1d5 (59), and Rin3 (60), or Sorting nexin 2 (Snx2) (59), which contains a phosphoinositide binding domain. Notably, the relocalization of intracellular vesicles containing signaling molecules has been shown to be required for antigen receptor signal propagation in T cells (61, 62). Future experiments will determine if PKD2-regulated phosphorylations influence the amplitude, location, and duration of T-cell signaling by controlling intracellular vesicle trafficking. Interestingly, among the PKD2 substrate candidates we also find GEF-H1 (*Arhgef2*), a microtubule-associated guanine nucleotide exchange factor whose function has been recently shown to be crucial for antiviral host defenses (63). In the context of phosphorylation and ubiquitylation crosstalk mentioned above, our study identified the E2 ubiquitin conjugating enzyme Ube2o which has a crucial role in endosomal protein trafficking (64) as novel PKD2 substrate in CTLs. Moreover the identification of the E3 ligase c-Cbl as a PKD2 substrate is also interesting, because c-Cbl is known to regulate the function and intracellular trafficking of several molecules implicated in antigen receptor signaling (50). Future studies into the role of PKD2 in regulating endosomal protein trafficking in CTLs may thus be interest.

Previous studies have shown that PKD2 has a critical role to control the T-cell transcriptional program. Antigen stimulation in CD8 T cells induces changes in the expression levels of ~2600 annotated genes and PKD2 both positively and negatively regulates expression of 5% this transcriptional program (5). Here we have identified PKD2 substrate candidates implicated in regulation of transcription and translation such as the Lysine (K)-specific demethylase 2a (Kdm2a) (51), the transcription factor NFAT3 (52) and Phax (53), a protein that controls mRNA export from the nucleus. However, the diversity of the PKD2 controlled phosphoproteome identified herein affords an explanation for the broad role of PKD2 as a regulator of the T-cell transcriptional program. Thus, there is no evidence for a simple linear pathway of phosphorylation of a single substrate that ex-

TABLE VII

PKD2 substrate candidates phosphosites. List of phosphosites from selected PKD2 substrate candidates, presented as gene name, protein name, modified position (Mod. Pos.) and SILAC ratio KO/WT (KO/WT ratio, averaged value of the three biological replicates)

Gene name	Protein name	Mod. Pos.	KO/WT Ratio
Akap10	A-kinase anchor protein 10, mitochondrial	S257	0.47
Arhgap11a	Rho GTPase-activating protein 11A	S847	0.51
Arhgef2	Rho guanine nucleotide exchange factor 2	S718	0.57
Arid4b	AT-rich interactive domain-containing protein 4B	S473	0.42
Arid5b	AT-rich interactive domain-containing protein 5B	S1002	0.20
Bud13	BUD13 homolog	S18	0.39
Casp8ap2	CASP8-associated protein 2	S1220	0.48
Cbl	E3 ubiquitin-protein ligase CBL	S617	0.57
Ccdc92	Coiled-coil domain-containing protein 92	S308	0.40
Dcaf5	DDB1- and CUL4-associated factor 5	S790	0.11
Dennd5a	DENN domain-containing protein 5A	S193	0.47
Dmwd	Dystrophia myotonica WD repeat-containing protein	T453	0.38
Fam76b	Protein FAM76B	S227	0.18
Hip1r	Huntingtin-interacting protein 1-related protein	S1045	0.13
Inpp4b	Type II inositol 3,4-bisphosphate 4-phosphatase	S470	0.23
Kansl3	KAT8 regulatory NSL complex subunit 3	S631	0.43
Kdm2a	Lysine-specific demethylase 2A	S422	0.29
Lrmp	Lymphoid-restricted membrane protein	S346	0.55
Lrrfip1	Leucine-rich repeat flightless-interacting protein 1	S284	0.56
Map4	Microtubule-associated protein 4	S973	0.48
Nfatc3	Nuclear factor of activated T-cells, cytoplasmic 3	S416	0.54
Nup214	Nuclear pore complex protein Nup214	S1029	0.37
Pcbp1	Poly(rC)-binding protein 1	S246	0.52
Phax	Phosphorylated adapter RNA export protein	S155	0.41
Plekha2	Pleckstrin homology domain-containing family A member 2	S349	0.45
Pola2	DNA polymerase alpha subunit B	S126	0.38
Prrc2a	Protein PRRC2A	S166	0.44
Ptpn22	Tyrosine-protein phosphatase non-receptor type 22	S452	0.52
Rdbp	Negative elongation factor E	S37	0.21
Reps1	RalBP1-associated Eps domain-containing protein 1	S475	0.50
Rin3	Ras and Rab interactor 3	S389	0.39
Rnf213	E3 ubiquitin-protein ligase RNF213	S4603	0.27
Sfr1	Swi5-dependent recombination DNA repair protein 1 homolog	S139	0.22
Snx2	Sorting nexin-2	S226	0.38
Supt16h	FACT complex subunit SPT16	S650	0.57
Tbc1d5	TBC1 domain family member 5	S546	0.45
Tsc2	Isoform E of Tuberin	S1254	0.52
Ube2o	Ubiquitin-conjugating enzyme E2 O	S394	0.40
Vps26b	Vacuolar protein sorting-associated protein 26B	S304	0.40
Wnk1	Serine/threonine-protein kinase WNK1	S2625	0.49
Znf687	Zinc finger protein 687	S1118	0.18
Znf687	Zinc finger protein 687	S495	0.43
Znf687	Zinc finger protein 687	S351	0.54

plains PKD2 action. Rather, the impact of PKD2 loss will thus result from a complex interplay between the direct and indirect effects of PKD2 loss on the phosphoproteome that are exposed by the present work.

A small number of the PKD2 substrates identified herein have been shown to be substrates for PKD family kinases in other cell lineages (Hip1r, Map4, Rdbp, Ssr3, Snx2, and Pcbp1). However, it is of equal importance to note that some of the key PKD substrates identified in experiments in fibroblasts, endothelial, and epithelial cells are not substrates in T cells. HDAC7 is thus a PKD substrate in many cells but not in CTLs, the protein phosphatase Slingshot (SSH1) is phosphorylated on Ser929 by PKD in HeLa and breast adenocarcinoma cell lines (6, 7) whereas the present data set revealed that SSH1 was phosphorylated on Ser929 in CTLs but this phosphorylation was not reduced on PKD2 null CTLs (supplemental Table S1). In the context of intracellular protein transport and Golgi function, other well described PKD substrates are the phosphatidylinositol-4 kinase III beta; a regulator of Golgi vesicle fission and protein secretion (9) and the lipid and sterol transfer proteins CERT and OSBP (10, 11). The present data identified eight unique phosphosites on phosphatidylinositol-4 kinase III beta (*Pi4kb*) including the Ser294, the PKD site previously characterized by Hausser and col-

leagues in fibroblast (9). We found that there was no reproducible loss of the phosphorylation of Phosphatidylinositol-4 kinase III beta in PKD2 null cells. Similarly, the ceramide transfer protein CERT (*Col4a3bp*) has been shown to be phosphorylated on Ser132 by PKD, thereby reducing its ceramide transfer activity and placing PKD as a regulator of lipid homeostasis. The phosphorylation of CERT of Ser132 was not reproducibly lost in PKD2 null CTLs making this an unlikely PKD2 substrate in CTLs.

Collectively, the data presented here show that PKD family kinases have both common and unique functions in different cell lineages. One explanation for this variability in substrates for different PKD isoforms could be that PKDs show cell lineage specific patterns of intracellular localization. For example in HEK293 and Hela cells PKD isoforms localize to the trans-Golgi network, where PKD phosphorylates substrates such as phosphatidylinositol-4 kinase III beta (9), CERT, and OSBP (10, 11). PKD1 has been also shown to be recruited to the lamellipodium in HEK293 cells and pancreatic tumor cell lines, where PKD phosphorylates substrates such as SSH1 (6, 7), cortactin (65), or Rin1 (8). In contrast, active PKD is mainly cytosolic in T cells (2). PKD is briefly recruited to the plasma membrane after antigen receptor stimulation but rapidly returns to the cytosol where it remains active (2). Thus, the cytosolic localization of PKD2 in T cells may prevent the access to substrates in particular cell compartments such as the Golgi network or the plasma membrane.

Acknowledgments—We thank members of the D.A.C. laboratory and S. Matthews for critical reading of the manuscript.

* This work was supported by the Wellcome Trust (065975/Z/01/A and 097418/Z/11Z to D.A.C.).

[S] This article contains supplemental Tables S1 to S4.

§ To whom correspondence should be addressed: Division of Cell Signalling and Immunology, University of Dundee, Dundee, DD1 5EH, Scotland, UK. Tel.: +44 (0)1382 385047; Fax: +44 (0)1382 385783; E-mail: d.a.cantrell@dundee.ac.uk.

¶ Present address: Instituto Investigación Sanitaria/Hospital Universitario de la Princesa, Universidad Autónoma de Madrid, Madrid, Spain.

‖Present address: Seidlstrasse 7, 82418 Murnau, Germany.

REFERENCES

1. Rozengurt, E. (2011) Protein kinase D signaling: multiple biological functions in health and disease. *Physiology* **26,** 23–33
2. Spitaler, M., Emslie, E., Wood, C. D., and Cantrell, D. (2006) Diacylglycerol and protein kinase D localization during T lymphocyte activation. *Immunity* **24,** 535–546
3. Wood, C. D., Marklund, U., and Cantrell, D. A. (2005) Dual phospholipase C/diacylglycerol requirement for protein kinase D1 activation in lymphocytes. *J. Biol. Chem.* **280,** 6245–6251
4. Matthews, S. A., Navarro, M. N., Sinclair, L. V., Emslie, E., Feijoo-Carnero, C., and Cantrell, D. A. (2010) Unique functions for protein kinase D1 and protein kinase D2 in mammalian cells. *Biochem. J.* **432,** 153–163
5. Navarro, M. N., Sinclair, L. V., Feijoo-Carnero, C., Clarke, R., Matthews, S. A., and Cantrell, D. A. (2012) Protein kinase D2 has a restricted but critical role in T-cell antigen receptor signalling in mature T-cells. *Biochem. J.* **442,** 649–659
6. Eiseler, T., Döppler, H., Yan, I. K., Kitatani, K., Mizuno, K., and Storz, P. (2009) Protein kinase D1 regulates cofilin-mediated F-actin reorganization and cell motility through slingshot. *Nat. Cell Biol.* **11,** 545–556
7. Peterburs, P., Heering, J., Link, G., Pfizenmaier, K., Olayioye, M. A., and Hausser, A. (2009) Protein kinase D regulates cell migration by direct phosphorylation of the cofilin phosphatase slingshot 1 like. *Cancer Res.* **69,** 5634–5638
8. Ziegler, S., Eiseler, T., Scholz, R.-P., Beck, A., Link, G., and Hausser, A. (2011) A novel protein kinase D phosphorylation site in the tumor suppressor Rab interactor 1 is critical for coordination of cell migration. *Mol. Biol. Cell* **22,** 570–580
9. Hausser, A., Storz, P., Märtens, S., Link, G., Toker, A., and Pfizenmaier, K. (2005) Protein kinase D regulates vesicular transport by phosphorylating and activating phosphatidylinositol-4 kinase IIIbeta at the Golgi complex. *Nat. Cell Biol.* **7,** 880–886
10. Fugmann, T., Hausser, A., Schöffler, P., Schmid, S., Pfizenmaier, K., and Olayioye, M. A. (2007) Regulation of secretory transport by protein kinase D-mediated phosphorylation of the ceramide transfer protein. *J. Cell Biol.* **178,** 15–22
11. Nhek, S., Ngo, M., Yang, X., Ng, M. M., Field, S. J., Asara, J. M., Ridgway, N. D., and Toker, A. (2010) Regulation of oxysterol-binding protein Golgi localization through protein kinase D-mediated phosphorylation. *Mol. Biol. Cell* **21,** 2327–2337
12. Matthews, S. A., Liu, P., Spitaler, M., Olson, E. N., McKinsey, T. A., Cantrell, D. A., and Scharenberg, A. M. (2006) Essential role for protein kinase D family kinases in the regulation of class II histone deacetylases in B lymphocytes. *Mol. Cell. Biol.* **26,** 1569–1577
13. Wang, Q. J. (2006) PKD at the crossroads of DAG and PKC signaling. *Trends Pharmacol. Sci.* **27,** 317–323
14. Rey, O., Sinnett-Smith, J., Zhukova, E., and Rozengurt, E. (2001) Regulated nucleocytoplasmic transport of protein kinase D in response to G protein-coupled receptor activation. *J. Biol. Chem.* **276,** 49228–49235
15. Marklund, U., Lightfoot, K., and Cantrell, D. (2003) Intracellular location and cell context-dependent function of protein kinase D. *Immunity* **19,** 491–501
16. Mayya, V., Lundgren, D. H., Hwang, S.-I., Rezaul, K., Wu, L., Eng, J. K., Rodionov, V., and Han, D. K. (2009) Quantitative phosphoproteomic analysis of T cell receptor signaling reveals system-wide modulation of protein-protein interactions. *Sci. Signal* **2,** ra46
17. Navarro, M. N., Goebel, J., Feijoo-Carnero, C., Morrice, N., and Cantrell, D. A. (2011) Phosphoproteomic analysis reveals an intrinsic pathway for the regulation of histone deacetylase 7 that controls the function of cytotoxic T lymphocytes. *Nat. Immunol.* **12,** 352–361
18. Ruperez, P., Gago-Martinez, A., Burlingame, A. L., and Oses-Prieto, J. A. (2012) Quantitative phosphoproteomic analysis reveals a role for serine and threonine kinases in the cytoskeletal reorganization in early T cell receptor activation in human primary T cells. *Mol. Cell Proteomics* **11,** 171–186
19. Franz-Wachtel, M., Eisler, S. A., Krug, K., Wahl, S., Carpy, A., Nordheim, A., Pfizenmaier, K., Hausser, A., and Macek, B. (2012) Global detection of protein kinase D-dependent phosphorylation events in nocodazole-treated human cells. *Mol. Cell Proteomics* **11,** 160–170
20. Sinclair, L. V., Finlay, D., Feijoo, C., Cornish, G. H., Gray, A., Ager, A., Okkenhaug, K., Hagenbeek, T. J., Spits, H., and Cantrell, D. A. (2008) Phosphatidylinositol-3-OH kinase and nutrient-sensing mTOR pathways control T lymphocyte trafficking. *Nat. Immunol.* **9,** 513–521
21. Cox, J., and Mann, M. (2008) MaxQuant enables high peptide identification rates, individualized p.p.b.-range mass accuracies and proteome-wide protein quantification. *Nat. Biotechnol.* **26,** 1367–1372
22. Cox, J., Neuhauser, N., Michalski, A., Scheltema, R. A., Olsen, J. V., and Mann, M. (2011) Andromeda: a peptide search engine integrated into the MaxQuant environment. *J. Proteome Res.* **10,** 1794–1805
23. Vizcaíno, J. A., Côté, R. G., Csordas, A., Dianes, J. A., Fabregat, A., Foster, J. M., Griss, J., Alpi, E., Birim, M., Contell, J., O'Kelly, G., Schoenegger, A., Ovelleiro, D., Pérez-Riverol, Y., Reisinger, F., Ríos, D., Wang, R., and Hermjakob, H. (2013) The PRoteomics IDEntifications (PRIDE) database and associated tools: status in 2013. *Nucleic Acids Res.* **41,** D1063–D1069
24. Huang, D. W., Sherman, B. T., and Lempicki, R. A. (2009) Systematic and integrative analysis of large gene lists using DAVID bioinformatics resources. *Nat. Protoc.* **4,** 44–57
25. Waugh, C., Sinclair, L., Finlay, D., Bayascas, J. R., and Cantrell, D. (2009) Phosphoinositide (3,4,5)-triphosphate binding to phosphoinositide-de-

pendent kinase 1 regulates a protein kinase B/Akt signaling threshold that dictates T-cell migration, not proliferation. *Mol. Cell. Biol.* **29,** 5952–5962
26. Cornish, G. H., Sinclair, L. V., and Cantrell, D. A. (2006) Differential regulation of T-cell growth by IL-2 and IL-15. *Blood* **108,** 600–608
27. Weninger, W., Crowley, M. A., Manjunath, N., and Andrian, von, U. H. (2001) Migratory properties of naive, effector, and memory CD8(+) T cells. *J. Exp. Med.* **194,** 953–966
28. Kalia, V., Sarkar, S., Subramaniam, S., Haining, W. N., Smith, K. A., and Ahmed, R. (2010) Prolonged interleukin-2Ralpha expression on virus-specific CD8+ T cells favors terminal-effector differentiation in vivo. *Immunity* **32,** 91–103
29. Pipkin, M. E., Sacks, J. A., Cruz-Guilloty, F., Lichtenheld, M. G., Bevan, M. J., and Rao, A. (2010) Interleukin-2 and inflammation induce distinct transcriptional programs that promote the differentiation of effector cytolytic T cells. *Immunity* **32,** 79–90
30. Malek, T. R., and Castro, I. (2010) Interleukin-2 receptor signaling: at the interface between tolerance and immunity. *Immunity* **33,** 153–165
31. Grønborg, M., Kristiansen, T. Z., Stensballe, A., Andersen, J. S., Ohara, O., Mann, M., Jensen, O. N., and Pandey, A. (2002) A mass spectrometry-based proteomic approach for identification of serine/threonine-phosphorylated proteins by enrichment with phospho-specific antibodies: identification of a novel protein, Frigg, as a protein kinase A substrate. *Mol. Cell Proteomics* **1,** 517–527
32. Huttlin, E. L., Jedrychowski, M. P., Elias, J. E., Goswami, T., Rad, R., Beausoleil, S. A., Villén, J., Haas, W., Sowa, M. E., and Gygi, S. P. (2010) A tissue-specific atlas of mouse protein phosphorylation and expression. *Cell* **143,** 1174–1189
33. Caenepeel, S., Charydczak, G., Sudarsanam, S., Hunter, T., and Manning, G. (2004) The mouse kinome: discovery and comparative genomics of all mouse protein kinases. *Proc. Natl. Acad. Sci. U.S.A.* **101,** 11707–11712
34. Tamas, P., Macintyre, A., Finlay, D., Clarke, R., Feijoo-Carnero, C., Ashworth, A., and Cantrell, D. (2010) LKB1 is essential for the proliferation of T-cell progenitors and mature peripheral T cells. *Eur. J. Immunol.* **40,** 242–253
35. Hardie, D. G., Ross, F. A., and Hawley, S. A. (2012) AMP-activated protein kinase: a target for drugs both ancient and modern. *Chem. Biol.* **19,** 1222–1236
36. Zarrouk, M., Rolf, J., and Cantrell, D. A. (2013) LKB1 mediates the development of conventional and innate T cells via AMP-dependent kinase autonomous pathways. *PLoS ONE* **8,** e60217
37. Matthews, S. A., Rozengurt, E., and Cantrell, D. (1999) Characterization of serine 916 as an in vivo autophosphorylation site for protein kinase D/Protein kinase Cmu. *J. Biol. Chem.* **274,** 26543–26549
38. Beadling, C., Ng, J., Babbage, J. W., and Cantrell, D. A. (1996) Interleukin-2 activation of STAT5 requires the convergent action of tyrosine kinases and a serine/threonine kinase pathway distinct from the Raf1/ERK2 MAP kinase pathway. *EMBO J.* **15,** 1902–1913
39. Ng, J., and Cantrell, D. (1997) STAT3 is a serine kinase target in T lymphocytes. Interleukin 2 and T cell antigen receptor signals converge upon serine 727. *J. Biol. Chem.* **272,** 24542–24549
40. Azzam, H. S., Grinberg, A., Lui, K., Shen, H., Shores, E. W., and Love, P. E. (1998) CD5 expression is developmentally regulated by T cell receptor (TCR) signals and TCR avidity. *J. Exp. Med.* **188,** 2301–2311
41. Spratley, S. J., Bastea, L. I., Döppler, H., Mizuno, K., and Storz, P. (2011) Protein kinase D regulates cofilin activity through p21-activated kinase 4. *J. Biol. Chem.* **286,** 34254–34261
42. Olayioye, M. A., Barisic, S., and Hausser, A. (2013) Multi-level control of actin dynamics by protein kinase D. *Cell. Signal.* **25,** 1739–1747
43. Nishikawa, K., Toker, A., Johannes, F. J., Songyang, Z., and Cantley, L. C. (1997) Determination of the specific substrate sequence motifs of protein kinase C isozymes. *J. Biol. Chem.* **272,** 952–960
44. Hutti, J. E., Jarrell, E. T., Chang, J. D., Abbott, D. W., Storz, P., Toker, A., Cantley, L. C., and Turk, B. E. (2004) A rapid method for determining protein kinase phosphorylation specificity. *Nat. Methods* **1,** 27–29
45. Döppler, H., Storz, P., Li, J., Comb, M. J., and Toker, A. (2005) A phosphorylation state-specific antibody recognizes Hsp27, a novel substrate of protein kinase D. *J. Biol. Chem.* **280,** 15013–15019
46. Parra, M., and Verdin, E. (2010) Regulatory signal transduction pathways for class IIa histone deacetylases. *Curr. Opin. Pharmacol.* **10,** 454–460
47. Parra, M., Kasler, H., McKinsey, T. A., Olson, E. N., and Verdin, E. (2005) Protein kinase D1 phosphorylates HDAC7 and induces its nuclear export after T-cell receptor activation. *J. Biol. Chem.* **280,** 13762–13770
48. Dequiedt, F., Van Lint, J., Lecomte, E., Van Duppen, V., Seufferlein, T., Vandenheede, J. R., Wattiez, R., and Kettmann, R. (2005) Phosphorylation of histone deacetylase 7 by protein kinase D mediates T cell receptor-induced Nur77 expression and apoptosis. *J. Exp. Med.* **201,** 793–804
49. Wang, Y., Waldron, R. T., Dhaka, A., Patel, A., Riley, M. M., Rozengurt, E., and Colicelli, J. (2002) The RAS effector RIN1 directly competes with RAF and is regulated by 14–3-3 proteins. *Mol. Cell. Biol.* **22,** 916–926
50. Balagopalan, L., Barr, V. A., and Samelson, L. E. (2009) Endocytic events in TCR signaling: focus on adapters in microclusters. *Immunol. Rev.* **232,** 84–98
51. Zhou, J. C., Blackledge, N. P., Farcas, A. M., and Klose, R. J. (2012) Recognition of CpG island chromatin by KDM2A requires direct and specific interaction with linker DNA. *Mol. Cell. Biol.* **32,** 479–489
52. Urso, K., Alfranca, A., Martínez-Martínez, S., Escolano, A., Ortega, I., Rodríguez, A., and Redondo, J. M. (2011) NFATc3 regulates the transcription of genes involved in T-cell activation and angiogenesis. *Blood* **118,** 795–803
53. Kitao, S., Segref, A., Kast, J., Wilm, M., Mattaj, I. W., and Ohno, M. (2008) A compartmentalized phosphorylation/dephosphorylation system that regulates U snRNA export from the nucleus. *Mol. Cell. Biol.* **28,** 487–497
54. Komander, D., and Rape, M. (2012) The ubiquitin code. *Annu. Rev. Biochem.* **81,** 203–229
55. Flotho, A., and Melchior, F. (2013) Sumoylation: a regulatory protein modification in health and disease. *Annu. Rev. Biochem.* **82,** 357–385
56. Hunter, T. (2007) The age of crosstalk: phosphorylation, ubiquitination, and beyond. *Mol. Cell* **28,** 730–738
57. Hay, R. T. (2013) Decoding the SUMO signal. *Biochem. Soc. Trans.* **41,** 463–473
58. Eggers, C. T., Schafer, J. C., Goldenring, J. R., and Taylor, S. S. (2009) D-AKAP2 interacts with Rab4 and Rab11 through its RGS domains and regulates transferrin receptor recycling. *J. Biol. Chem.* **284,** 32869–32880
59. Seaman, M. N. J., Harbour, M. E., Tattersall, D., Read, E., and Bright, N. (2009) Membrane recruitment of the cargo-selective retromer subcomplex is catalysed by the small GTPase Rab7 and inhibited by the Rab-GAP TBC1D5. *J. Cell Sci.* **122,** 2371–2382
60. Kajiho, H., Sakurai, K., Minoda, T., Yoshikawa, M., Nakagawa, S., Fukushima, S., Kontani, K., and Katada, T. (2011) Characterization of RIN3 as a guanine nucleotide exchange factor for the Rab5 subfamily GTPase Rab31. *J. Biol. Chem.* **286,** 24364–24373
61. Larghi, P., Williamson, D. J., Carpier, J.-M., Dogniaux, S., Chemin, K., Bohineust, A., Danglot, L., Gaus, K., Galli, T., and Hivroz, C. (2013) VAMP7 controls T cell activation by regulating the recruitment and phosphorylation of vesicular Lat at TCR-activation sites. *Nat. Immunol.* **14,** 723–731
62. Soares, H., Henriques, R., Sachse, M., Ventimiglia, L., Alonso, M. A., Zimmer, C., Thoulouze, M.-I., and Alcover, A. (2013) Regulated vesicle fusion generates signaling nanoterritories that control T cell activation at the immunological synapse. *J. Exp. Med.* **210,** 2415–2433
63. Chiang, H.-S., Zhao, Y., Song, J.-H., Liu, S., Wang, N., Terhorst, C., Sharpe, A. H., Basavappa, M., Jeffrey, K. L., and Reinecker, H.-C. (2013) GEF-H1 controls microtubule-dependent sensing of nucleic acids for antiviral host defenses. *Nat. Immunol*, **15,** 63–71
64. Hao, Y.-H., Doyle, J. M., Ramanathan, S., Gomez, T. S., Jia, D., Xu, M., Chen, Z. J., Billadeau, D. D., Rosen, M. K., and Potts, P. R. (2013) Regulation of WASH-dependent actin polymerization and protein trafficking by ubiquitination. *Cell* **152,** 1051–1064
65. Eiseler, T., Hausser, A., De Kimpe, L., Van Lint, J., and Pfizenmaier, K. (2010) Protein kinase D controls actin polymerization and cell motility through phosphorylation of cortactin. *J. Biol. Chem.* **285,** 18672–18683